Medicinal Chemistry Research (2019) 28:768–777
https://doi.org/10.1007/s00044-019-02333-5

MEDICINAL CHEMISTRY RESEARCH

ORIGINAL RESEARCH

Check for updates

Synthesis and antitumor activity of cyclic octapeptide, samoamide A, and its derivatives

Fei Ge[1] · Chi Zhang[1] · Longbao Zhu[1] · Wanzhen Li[1] · Ping Song[1] · Yugui Tao[1] · Guocheng Du[2]

Received: 1 January 2019 / Accepted: 5 March 2019 / Published online: 26 March 2019
© Springer Science+Business Media, LLC, part of Springer Nature 2019

Abstract

Using 2-chloro-trityl chloride resin as a solid phase carrier, a linear peptide was synthesized by Fmoc solid phase synthesis followed by liquid phase cyclization. After separation and purification by high-performance liquid chromatography (HPLC), cyclic octapeptide samoamide A was prepared. The synthesis yield was 54.5%. The structure of cyclic octapeptide samoamide A was characterized by electrospray ionization–mass spectrometry (ESI-MS) and nuclear magnetic resonance (NMR) spectrometry. The biological activity was evaluated by the CCK-8 assay and DPP4 enzyme activity inhibition assay. This compound exhibited high antitumor activity. Using samoamide A as a lead compound, eight cyclic octapeptide samoamide A derivatives (a, b, c, d, e, f, g, and h) were designed and synthesized using the alanine scanning method. The molecular weight and chemical structure of these derivatives were verified by ESI-MS and NMR, and the antitumor activity of the derivatives was analyzed. The antitumor activity of compound f was similar to that of samoamide A, and its replacement site is the non-active site of samoamide A, providing a theoretical basis for further modification and transformation of samoamide A.

Keywords Samoamide A · Samoamide A derivatives · Solid phase synthesis · Alanine scanning method · Antitumor activity · Non-active site

Introduction

Malignant tumors are a serious threat to human life and health and cause high morbidity and mortality worldwide (Al-Benna et al. 2011; Andrade et al. 2018; Khalily et al. 2018). Because of their low toxicity, clear target specificity, and small molecular weight, peptide drugs have gained attention in the research and development of antitumor drugs (Rosca et al. 2011). In recent years, researchers have identified a variety of small molecular peptides with antitumor activity, such as the integrin antagonist AP25 with the function of antiangiogenesis, NC1(XIX)-F4 with antitumor activity released by plasmin, and TZT-1027 and Kahalalide F, which have relatively strong killing effects on non-small cell lung cancer cells and melanoma cells, respectively (Hu et al. 2015; Oudart et al. 2015; Riely et al. 2007; Martin-Algarra et al. 2009). Currently, marine organisms have become recognized as promising resources for natural products with biological activity, particularly peptide analogs with good biological activity extracted from sponge and cyanobacteria (Aneiros and Garateix 2004; Gogineni and Hamann 2018).

Increasing attention has been given to cyclic peptide compounds with a wide range of biological activities. Compared to linear peptides, cyclic peptide compounds have advantages such as stable structures, high fat solubility, strong membrane penetrating ability, and long half-life period in vivo (Abdalla 2016; Dartois et al. 2005). Their biological activities can be further improved by chemically

These authors contributed equally: Fei Ge, Chi Zhang

Supplementary information The online version of this article (https://doi.org/10.1007/s00044-019-02333-5) contains supplementary material, which is available to authorized users.

✉ Yugui Tao
swgctaoyg@126.com

✉ Guocheng Du
gcdu@jiangnan.edu.cn

[1] School of Biochemical Engineering, Anhui Polytechnic University, Beijing Middle Road, 241000 Wuhu, Anhui, P. R. China

[2] Key Laboratory of Industrial Biotechnology, Ministry of Education, School of Biotechnology, Jiangnan University, 214122 Wuxi, Jiangsu, P. R. China

modifying the cyclic peptide (Johnstone et al. 2005). Common polypeptide modification methods include backbone end modification, side chain modification, and amino acid substitution (Riahi et al. 2017; Mccusker et al. 2002). By replacing amino acids in the polypeptide with alanine in sequence to investigate the effect of amino acid changes at different sites on the biological activity of the cyclic peptide, the replacement with alanine removes the active group on the side chain and replaces it with a small methyl group with no other functional groups, which has little effect on the protein structure, alanine scanning technology can provide a basis for structural transformation of cyclic peptide compounds (Miyake et al. 2002).

Samoamide A is a cyclic peptide extracted from *Symploca* sp. collected in American Samoan. It has shown good cytotoxicity in in vitro activity tests, with an IC_{50} value of <10 μM against colorectal cancer cells and between 1.1 and 4.5 μM against non-small lung cancer cells, breast cancer cells, and others (Naman et al. 2017; Chang et al. 2018). However, the samoamide A content in natural products is very low and cannot satisfy the demand for studying in structure–activity relationship, which limits its further development and applications. Solid phase synthesis of peptides has the advantages of short synthesis time, low cost and simple operation, and liquid phase cyclization can effectively improve the yield. In this study, samoamide A was synthesized by solid phase synthesis, liquid phase cyclization, and its structure was characterized. The alanine scanning method was used to identify the inactive site of samoamide A, which provides a theoretical basis for subsequent modification and transformation of samoamide A (Lim et al. 2006; Li et al. 2017).

Materials and methods

Materials and instruments

N-Fluorenyl-9-methoxycarbonyl (Fmoc) protected L-amino acids: Fmoc-Phe-OH, Fmoc-Ile-OH, Fmoc-Pro-OH, Fmoc-Leu-OH, Fmoc-Val-OH, 2-chloro-trityl chloride resin (with a loading amount of 0.985 mmol/g), 2-(7-azabenzotriazol-1-yl)-*N*,*N*,*N*',*N*'-tetramethyluronium hexafluorophosphate (HATU), 1-hydroxybenzotriazole (HOBt), and benzotriazol-1-yl-oxytripyrrolidinophosphonium hexafluorophosphate (PyBOP) were purchased from GL Biochem (Shanghai) Ltd. (Shanghai, China); LH-20 was purchased from Guangzhou Qiyun Biotechnology Co., Ltd. (Guangdong, China); dichloromethane (DCM), *N*,*N*-diisopropylethylamine (DIPEA), trifloro acetic acid (TFA), and dimethylformamide (DMF) were obtained by Shanghai Reagent Chemical Co. (Shanghai, China) and used directly. Dipeptidyl peptidase-4 (DPP4) inhibitor and the CCK-8 value-added test kit were purchased from Shanghai Tongren Group (Shanghai, China); phosphate buffer solution, 0.25% trypsin, penicillin–streptomycin solution, and fetal bovine serum were purchased from Invitrogen (Carlsbad, CA, USA). 4T1 cells were obtained from the Cell Bank of the Chinese Academy of Science.

A Bruker Spectmspin AC-P600 nuclear magnetic resonance spectrometer (Bruker Corporation, Germany), LC-20A high-performance liquid chromatograph (Shimadzu, Japan), LCMS-8030 three-quadrupole mass spectrometer (Shimadzu, Japan), Synergy NEO microplate reader of multi-wavelength (BioTek, USA), and a DFY-5/25 low-temperature constant temperature reaction apparatus (Changzhou Nuoji Instrument Co. Ltd., China) were used.

Preparation of test reagents

Six grams of ninhydrin was weighed and dissolved in 100 mL of absolute ethanol; 20 mL of absolute ethanol was added to 80 mL of phenol solution. These solutions and 50 mL of pyridine were separately poured into three 100-mL brown glass bottles.

Synthesis route of samoamide A

The synthesis route of samoamide A is shown in Fig. 1.

Activation of 2-chloro-trityl chloride resin

First, 2.00 g of 2-chloro-trityl chloride resin was added to the polypeptide synthesis tube and rinsed once with DMF and DCM. After suction filtration, approximately 30 mL of DCM was added so that the chlorine resin fully swelled for 1 h; subsequently, the resin was drained using a water pump.

Synthesis of Fmoc-Phe-Resin (1)

As shown in step (A) of Fig. 1, 1029.4 mg of Fmoc-Phe-OH was added to a sand core tube, DCM and 1390 μL of DIPEA were used as the solvent and condensation reagent, respectively, and air was pumped to perform bubbling reaction for 1 h at 25 °C. After draining the solvent, DCM and DFM were used to rinse the solid three times. Thirty milliliters of 25% methanol/DCM (V/V) solution was added to react for 30 min, and then the residual active sites of the resin were blocked. The solvent was drained, DMF was used to rinse the solid three times, and Fmoc-Phe-Resin (1) was obtained.

Synthesis of Phe-Resin (2)

The synthesis route is shown in step (B) of Fig. 1. First, 30 mL of 25% piperidine/DMF (V/V) solution was added to a

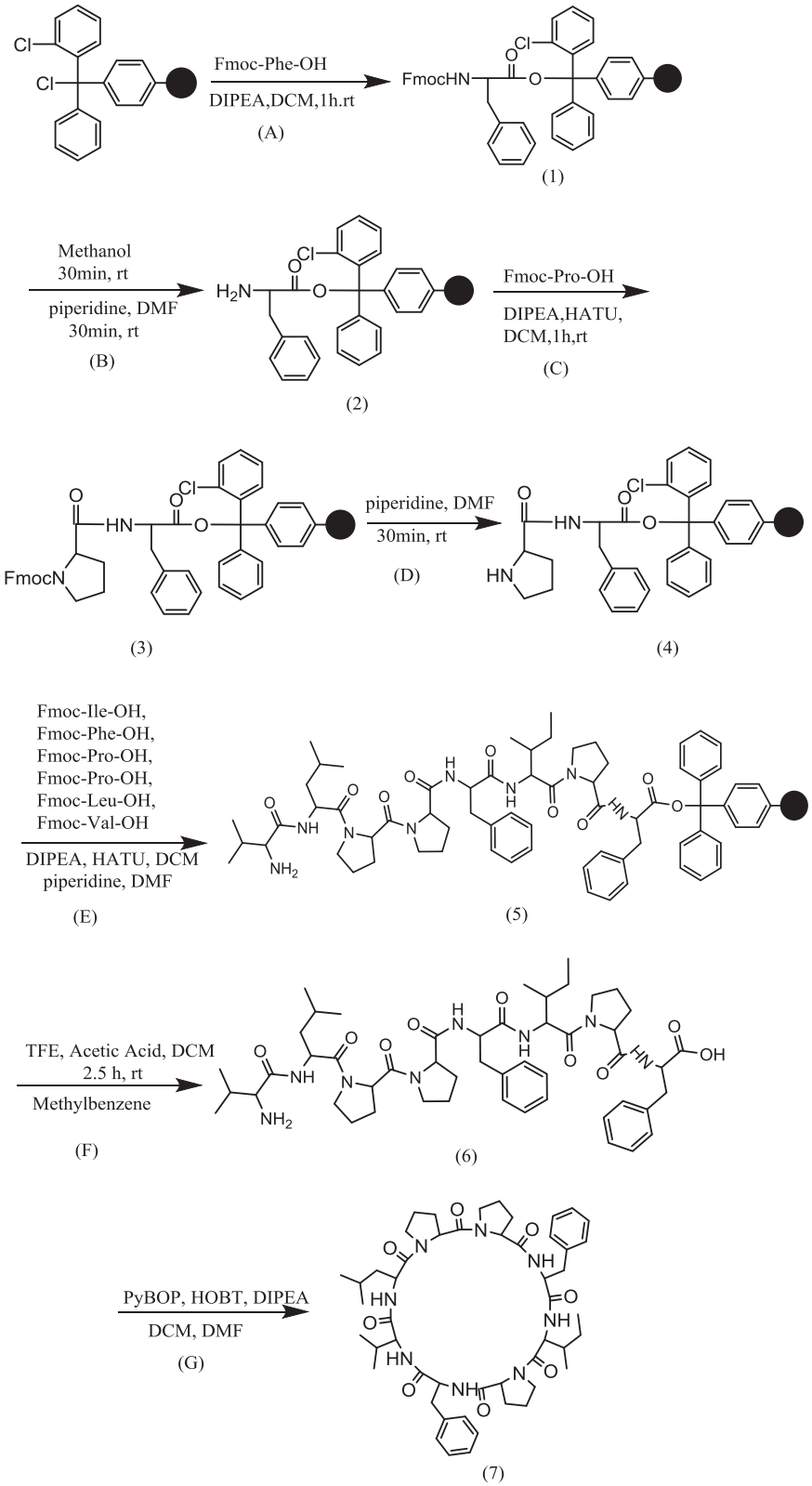

Fig. 1 Synthesis route of samoamide A

sand core reaction tube, subjected to a bubbling reaction by pumping air into the solution for 30 min, and followed by the de-Fmoc reaction. After the reaction, the solvent was drained and the residue was rinsed five times with DCM and DMF.

Ninhydrin color development detection

More than 10 pieces of amino resin were randomly removed and placed into the test tube. The detection reagents, comprising of 6% ninhydrin ethanol solution, 80% phenol ethanol solution, and pyridine in the volume ratio of 2:1:1, were added and heated at 100 °C for 2 min. The color of the resin was observed. A dark blue color of the resin indicated that the intermediate (2) was obtained, and the next reaction could be carried out.

Synthesis of linear peptide NH2-Val-Leu-Pro-Pro-Phe-Ile-Pro-Phe-Resin (5)

The synthesis route is shown in step (C) of Fig. 1. First, 2692.5 mg of Fmoc-Pro-OH, 1390 µL DIPEA, 1517 mg HATU, and 20 mL DCM were added to a reaction tube for 1 h at 25 °C. The reaction solution was drained, and DCM and DMF were used to rinse the mixture three times, after which the rinsing solution was drained. Ninhydrin color development detection was conducted as described above. If the color remained unchanged, it indicated that the intermediate (3) was synthesized successfully. Otherwise, the above reaction was repeated until intermediate (3) was successfully synthesized. Next, the de-Fmoc reaction was carried out as shown in step (D) of Fig. 1 in which the intermediate (4) was obtained. The above experimental procedures were repeated, and amino acids were sequentially added to obtain the intermediate (5).

Synthesis of linear peptide NH2-Val-Leu-Pro-Pro-Phe-Ile-Pro-Phe-OH (6)

The amino acid resin was transferred into a 50 mL centrifuge tube, and 30 mL of 95% TFA cutting solution was added for oscillatory reaction for 2.5 h at 25 °C. The filtrate solution was suction-filtered into a 100 mL eggplant-shaped bottle. The mixture was dehydrated under reduced pressure using a water pump to remove DCM from the filtrate and concentrated under reduced pressure with an oil pump. Diethyl ether was added at a volume ratio of 1:4, and the mixture was centrifuged to obtain a white solid, which was a crude linear peptide of NH_2-Val-Leu-Pro-Pro-Phe-Ile-Pro-Phe-OH.

The crude linear peptide was dissolved in methanol and purified by high-performance liquid chromatography (HPLC). Acetonitrile containing 0.1% TFA and water containing 0.1% TFA was used as the eluent with a detection wavelength of 254 nm, C_{18} reverse column as the preparation column, and the following gradient settings of the mobile phase: 0–15 min, acetonitrile 20–80%; 15–30 min, acetonitrile 80–95%.

Synthesis of samoamide A (7)

First, 100 mg of pure linear peptide (6) was dissolved in 100 mL of anhydrous DCM and placed in a constant pressure dropping funnel. Next, 280.2 mg of PyBOP, 72.8 mg of HOBt, and 188 µL of DIPEA were dissolved in 100 mL of anhydrous DCM, and the mixture was transferred into a round-bottom flask. The above device was evacuated, protected with argon gas, and placed in ice water at 0 °C. The solution in the constant pressure dropping funnel was slowly added in a dropwise manner and completed in 4 h, and the reaction was conducted overnight at 25 °C.

The solvent was evaporated under reduced pressure, and then the mixture was purified by a Sephadex LH-20 column to obtain cyclic peptide samoamide A solution. The solution and filtrate were concentrated under reduced pressure using a pump to remove DCM from the filtrate and obtain a light yellow powdery solid, which was a crude product of samoamide A (7).

The crude cyclic peptide was dissolved in methanol and further separated and purified by HPLC, after which the target peak solution was collected. After cryodesiccation, a white powdery solid was obtained. The molecular weight and the structure of the compound were determined by electrospray ionization–mass spectrometry (ESI-MS) and nuclear magnetic resonance (NMR) spectrometry. The analytical conditions of ESI-MS were as follows: ion source: ESI(+), scan target product with SIM pattern, scanning range (*m*/*z*): 800–860, temperature at the interface: 300 °C, temperature at the DL: 250 °C, temperature of the heat block: 400 °C, drying gas flow: 15 L/min, voltage at capillary: 4500 V, detection voltage: 1960 V. The analytical conditions of NMR were as follows: the sample was dissolved in methanol. The height of the sample volume was approximately 4 cm in the NMR tube, volume was 0.5 mL, and the sample amount was as follows: 1H: approximately 5–10 mg, 13C: >20 mg. The sweeping range of NMR was set at 1H: −2 to 13 ppm, 13C: −20 to 230 ppm, SF (^{1}H): 400 MHz, and SF (^{13}C): 100 MHz.

Alanine scanning of samoamide A

The synthesis method was the same as that described above. The eight amino acids of the cyclic peptide, samoamide A, were sequentially replaced with alanine so that eight new cyclic peptides (a, b, c, d, e, f, g, and h) were synthesized, the structures of which are shown in Fig. 2. ESI-MS and

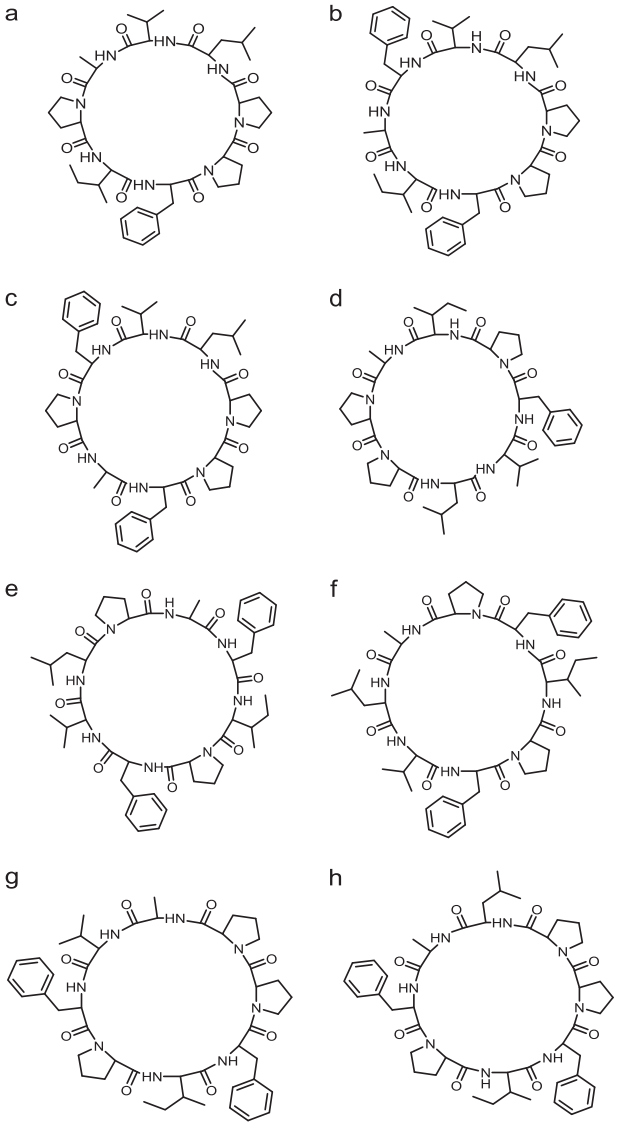

Fig. 2 Structure diagram of the samoamide A derivatives

NMR were conducted to determine the molecular weights and structures of the obtained derivatives of samoamide A.

Cytotoxicity test

The effect of the sample on the toxicity of 4T1 cells was examined by the CCK-8 method. The examination method is referred to the literature (Li et al. 2015). 4T1 cells were cultured according to the standard cell culture method (Yi et al. 2015). 4T1 cells were incubated until 90% of the cells were in an adherent state, which were then digested with 1 mL of 0.25% trypsin in an incubator for 2 min and centrifuged at 800 r/min for 5 min. After the cells were resuspended in a complete medium, the number of cells was determined with a hemocytometer, and the concentration of the resuspended 4T1 cell solution was diluted to 8×10^4/ mL. Next, 100 µL of the cell suspension was pipetted into 96-well plates (approximately 8000 cells/well), which were placed in a constant temperature CO_2 incubator and incubated until the cells were in an adherent state. Peptide solutions of 0, 3.125, 6.25, 12.5, 25, and 50 µg/mL were added. After culturing for 24 h, the cells were observed by an inverted microscope. After removing the original culture solution, 100 µL of cell culture medium containing 0.09% CCK-8 was added to each well and the cells were incubated for 2 h. The absorbance of each well was measured at 450 nm by a full-functional microplate reader.

DPP4 enzyme activity inhibition experiment

The DPP4 inhibitory activity of the sample solution was tested using a DPP4 Inhibitor Test Kit. First, 49 µL of test buffer and 1 µL of DPP4 enzyme solution were added to each well of the 96-well enzyme-linked immunosorbent assay plates; a blank control well, sample well to be tested, and inhibitor control well were used. The blank control well contained no substance. The inhibitor control well contained 2 µL of the inhibitor sitagliptin mother solution provided by the test kit and diluted by 100-fold with the test buffer. Next, 25 µL of the diluted solution was removed and added to the inhibitor control well. For the test sample, 25 µL of polypeptide sample solution at concentrations of 100, 10, 1, 0.1, and 0.01 µg/mL was added. The sample was incubated at 37 °C for 10 min; 23 µL of test buffer solution and 2 µL of DPP4 substrate were added to each well and mixed with a pipette. The sample was incubated for another 10 min; a full-functional microplate reader was used to measure the absorbance of the sample at 37 °C and protected from light, with an excitation wavelength of 360 nm and absorption wavelength of 460 nm (Schubert et al. 2002; Valeriote et al. 2012).

Results and discussion

Synthesis of samoamide A

ESI-MS revealed that the $[M+H]^+$ (m/z) of the linear peptide of NH_2-Val-Leu-Pro-Pro-Phe-Ile-Pro-Phe-OH (6) was 929.60, which is consistent with the theoretical molecular weight 928.54; the nuclear magnetic spectrum was consistent with the theoretical structure. After 2.00 g of the synthesized product of 2-chloro-trityl chloride resin was purified with an HPLC preparation column, 250.0 mg of intermediate (6) was obtained in a yield of 85.9%.

After 100 mg of the linear peptide (6) was introduced, 54.5 mg of samoamide A was obtained after the cyclization product was purified by HPLC with a yield of 54.5% and purity of 95.8%.

Table 1 ESI-MS data of samoamide A and derivatives

Compound	HRMS, *m/z* $[M+1]^+$	M
Samoamide A	911.35	910.50
a	835.50	834.50
b	885.50	884.52
c	869.50	868.48
d	835.50	834.51
e	885.55	884.53
f	885.55	884.53
g	869.50	868.48
h	883.50	882.51

ESI-MS electrospray ionization–mass spectrometry

The MS results of samoamide A and the compounds a, b, c, d, e, f, g, and h prepared by alanine scanning are shown in Table 1.

Spectral data for samoamide A

^{1}H NMR (400 MHz, MeOD): δ 7.45–7.23 (m, 10H, ArH), 4.71 (t, 1H, $J = 12.0$ Hz, NCHCO), 4.50–4.31 (m, 3H, NCHCO), 4.27–4.15 (m, 4H, NCHCO), 3.91–3.63 (m, 6H, CH_2), 3.60–3.11 (m, 4H, CH_2), 2.28–2.13 (m, 3H, CCH), 2.12–1.56 (m, 16H, CCH_2), 1.48–0.83 (m, 18H, CCH_3). ^{13}C NMR (100 MHz, MeOD): δ 173.75, 172.64, 172.54, 171.91, 171.72, 171.50, 171.42, 170.13, 137.87, 136.72, 128.90, 128.69, 128.46, 128.20, 127.01, 126.54, 61.55, 61.53, 60.68, 60.54, 59.58, 57.81, 55.11, 50.04, 48.29, 48.26, 48.05, 47.84, 47.63, 47.41, 47.20, 46.98, 46.46, 41.12, 38.06, 37.26, 34.84, 31.82, 31.00, 29.25, 27.88, 25.18, 24.65, 24.56, 24.05, 22.62, 20.90, 20.77, 18.17, 18.13. ESI-MS revealed that the $[M+H]^+$ (*m/z*) of samoamide A was 911.35, which is consistent with the theoretical molecular weight 910.50.

Spectral data for compound a

^{1}H NMR (400 MHz, MeOD): δ 8.17 (d, 1H, $J = 7.6$ Hz, NH), 8.13 (d, 1H, $J = 8.8$ Hz, NH), 7.74 (d, 1H, $J = 9.6$ Hz, NH), 7.70 (d, 1H, $J = 6.4$ Hz, NH), 7.39–7.32 (m, 2H, ArH), 7.31–7.21 (m, 3H, ArH), 4.65 (t, 1H, $J = 10.0$ Hz, NCHCO), 4.44–4.32 (m, 2H, NCHCO), 4.28–4.05 (m, 2H, NCHCO), 3.99–3.77 (m, 3H, NCHCO), 3.76–3.62 (m, 2H, CH_2), 3.50–3.39 (m, 1H, CH_2), 3.29–3.01 (m, 3H, CH_2), 2.38–2.13 (m, 3H, CCH), 2.12–1.50 (m, 18H, CH_3), 1.38–0.89 (m, 21H, CH_3). ^{13}C NMR (100 MHz, MeOD): δ 175.04, 174.76, 174.68, 174.12, 173.20, 173.09, 173.03, 172.79, 171.46, 138.05, 130.09, 129.84, 128.43, 63.72, 62.64, 62.12, 60.98, 59.23, 56.58, 54.65, 51.27, 49.64, 49.43, 49.21, 48.79, 48.57, 48.36, 42.54, 39.16, 38.55, 33.56, 32.51, 30.58, 29.34, 26.44, 25.97, 25.87, 25.38, 23.91, 22.37, 22.17, 19.49, 19.30, 17.05, 16.18, 11.40. ESI-MS revealed that the $[M+H]^+$ (*m/z*) of compound a was 835.5, which is consistent with the theoretical molecular weight 834.50.

Spectral data for compound b

^{1}H NMR (400 MHz, MeOD): δ 7.37–7.18 (m, 10H, ArH), 4.49–4.34 (m, 2H, NCHCO), 4.25 (d, 1H, $J = 12.0$ Hz, NCHCO), 4.19–4.05 (m, 2H, NCHCO), 3.90–3.79 (m, 1H, NCHCO), 3.71–3.61 (m, 2H, CH), 3.60–3.41 (m, 2H, CH_2), 3.34–3.28 (m, 2H, CH_2), 3.27–2.94 (m, 4H, CH_2), 2.19–1.78 (m, 8H, CCH_2), 1.64–1.30 (m, 4H, CCH_2), 1.16–0.91 (m, 21H, CH_3). ^{13}C NMR (100 MHz, MeOD): δ 176.58, 176.10, 174.68, 174.24, 173.92, 173.40, 173.32, 173.30, 172.94, 172.92, 172.52, 171.51, 171.21, 139.08, 138.18, 130.34, 130.03, 129.85, 129.58, 128.35, 127.94, 120.06, 62.76, 62.04, 61.74, 61.00, 59.16, 58.74, 52.69, 51.52, 51.41, 50.42, 50.02, 49.64, 49.43, 49.21, 48.79, 48.57, 48.36, 47.80, 42.53, 39.51, 38.70, 36.39, 32.96, 32.20, 29.24, 26.60, 26.10, 25.62, 24.03, 22.23, 19.68, 19.39, 16.44, 16.10, 11.48. ESI-MS revealed that the $[M+H]^+$ (*m/z*) of compound b was 885.50, which is consistent with the theoretical molecular weight 884.52.

Spectral data for compound c

^{1}H NMR (400 MHz, MeOD): δ 7.34–7.16 (m, 10H, ArH), 4.79–4.22 (m, 8H, NCHCO), 3.92–3.52 (m, 6H, CH_2), 3.27–2.97 (m, 4H, CH_2), 2.35–2.17 (m, 2H, CCH), 2.16–1.49 (m, 14H, CCH_2), 1.32–0.92 (m, 15H, CH_3). ^{13}C NMR (100 MHz, MeOD): δ 174.35, 173.98, 173.08, 173.06, 172.69, 172.66, 172.34, 172.20, 171.55, 169.59, 139.01, 138.28, 138.09, 130.60, 130.44, 130.40, 130.22, 129.59, 129.47, 129.43, 127.82, 61.56, 61.40, 59.71, 59.42, 55.64, 55.00, 51.18, 49.43, 49.22, 48.80, 48.37, 38.36, 38.28, 31.62, 31.53, 30.14, 29.35, 25.94, 25.74, 23.66, 21.92, 21.80, 19.44, 18.91, 17.82, 17.22. ESI-MS revealed that the $[M+H]^+$ (*m/z*) of compound c was 869.50, which is consistent with the theoretical molecular weight 868.48.

Spectral data for compound d

^{1}H NMR (400 MHz, MeOD): δ 7.36–7.20 (m, 5H, ArH), 4.77–4.69 (m, 1H, NCHCO), 4.68–4.60 (m, 1H, NCHCO), 4.38 (dd, 1H, $J = 8.0$, 4.0Hz, NCHCO), 4.24–4.11 (m, 2H, NCHCO), 4.05 (dd, 1H, $J = 8.0$, 4.0 Hz, NCHCO), 3.90–3.81 (m, 2H, CH), 3.80–3.57 (m, 5H, CH_2), 3.54–3.35 (m, 2H, CH_2), 3.25 (dd, 2H, $J = 12.0$, 4.0 Hz, CH_2), 2.35–2.16 (m, 3H, CCH), 2.09–1.51 (m, 16H, CCH_2), 1.36–0.89 (m, 21H, CH_3). ^{13}C NMR (100 MHz, MeOD): δ 175.55, 174.97, 173.91, 173.57, 173.20, 173.16, 173.07, 172.95,

171.03, 139.32, 130.29, 129.59, 127.91, 63.09, 62.15, 61.61, 60.84, 56.16, 56.06, 54.21, 51.33, 51.22, 49.64, 49.43, 49.21, 48.79, 48.57, 48.36, 42.27, 36.15, 33.39, 33.03, 30.63, 29.42, 26.27, 25.89, 25.83, 25.15, 23.77, 22.35, 19.55, 17.70, 16.26, 11.27. ESI-MS revealed that the $[M+H]^+$ (*m/z*) of compound d was 835.50, which is consistent with the theoretical molecular weight 834.51.

Spectral data for compound e

^{1}H NMR (400 MHz, MeOD): δ 7.36–7.12 (m, 10H, ArH), 4.81–4.58 (m, 2H, NCHCO), 4.55–3.88 (m, 6H, NCHCO), 3.85–3.37 (m, 5H, CH_2), 3.30–2.91 (m, 3H, CH_2), 2.36–2.09 (m, 3H, CCH), 1.94–1.32 (m, 12H, CCH_2), 1.28–0.84 (m, 21H, CH_3). ^{13}C NMR (100 MHz, MeOD): δ 181.08, 180.51, 176.41, 166.32, 148.47, 139.17, 138.61, 138.42, 138.32, 137.74, 137.57, 135.96, 135.81, 135.59, 71.18, 70.45, 69.74, 66.30, 63.64, 63.21, 62.20, 61.70, 61.41, 59.50, 57.50, 56.27, 55.49, 49.50, 49.33, 49.17, 48.83, 48.67, 48.50, 44.64, 40.82, 38.56, 38.36, 36.08, 34.71, 33.96, 32.67, 32.60, 32.12, 29.18, 28.35, 24.33, 20.69, 20.59. ESI-MS revealed that the $[M+H]^+$ (*m/z*) of compound e was 885.55, which is consistent with the theoretical molecular weight 884.53.

Spectral data for compound f

^{1}H NMR (400 MHz, MeOD): δ 7.39–7.18 (m, 10H, ArH), 4.79–4.46 (m, 4H, NCHCO), 4.42–4.21 (m, 2H, NCHCO), 4.08–3.87 (m, 2H, NCHCO), 3.86–3.56 (m, 4H, CH_2), 3.46–3.35 (m, 1H, CH_2), 3.29–2.97 (m, 3H, CH_2), 2.18–1.95 (m, 3H, CCH), 1.94–1.28 (m, 12H, CCH_2), 1.28–0.83 (m, 21H, CH_3). ^{13}C NMR (100 MHz, MeOD): δ 174.71, 174.01, 173.82, 173.73, 173.32, 173.24, 172.88, 172.80, 172.66, 139.60, 138.12, 130.22, 130.10, 129.80, 129.52, 128.42, 127.79, 101.37, 62.94, 62.79, 62.05, 60.97, 58.95, 56.55, 52.92, 49.65, 49.43, 49.22, 48.79, 48.58, 48.37, 47.82, 42.32, 39.09, 35.88, 33.53, 32.40, 30.57, 26.43, 25.32, 24.21, 22.12, 22.06, 19.49, 19.41, 16.31, 15.75, 11.46. ESI-MS revealed that the $[M+H]^+$ (*m/z*) of compound f was 885.55, which is consistent with the theoretical molecular weight 884.53.

Spectral data for compound g

^{1}H NMR (400 MHz, MeOD): δ 7.39–7.20 (m, 10H, ArH), 4.67 (t, 2H, $J = 12.0$ Hz, NCHCO), 4.45–4.29 (m, 2H, NCHCO), 4.18–4.04 (m, 2H, NCHCO), 3.91–3.82 (m, 2H, NCHCO), 3.81–3.54 (m, 4H, CH_2), 3.52–3.38 (m, 1H, CH_2), 3.33–3.02 (m, 5H, CH_2), 2.26–2.10 (m, 2H, CCH), 2.05–1.37 (m, 14H, CCH_2), 1.35–0.63 (m, 15H, CCH_3). ^{13}C NMR (100 MHz, MeOD): δ 175.51, 175.43, 175.40, 174.29, 174.18, 174.05, 173.59, 173.56, 173.47, 173.09, 172.99, 172.87, 172.05, 172.02, 139.07, 138.12, 130.28, 130.02, 129.92, 129.61, 128.35, 127.97, 62.87, 62.70, 62.18, 62.00, 60.95, 59.13, 56.45, 49.68, 49.64, 49.43, 49.21, 48.79, 48.69, 48.57, 48.36, 47.89, 39.62, 38.46, 36.29, 33.02, 32.40, 30.62, 29.24, 25.99, 25.43, 22.16, 19.54, 19.50, 17.00, 15.91, 11.21. ESI-MS revealed that the $[M+H]^+$ (*m/z*) of compound g was 869.50, which is consistent with the theoretical molecular weight 868.48.

Spectral data for compound h

^{1}H NMR (400 MHz, MeOD): δ 7.40–7.19 (m, 10H, ArH), 4.72–4.63 (m, 4H, NCHCO), 4.45–4.29 (m, 3H, NCHCO), 4.22–4.04 (m, 1H, NCHCO), 3.86–3.45 (m, 6H, CH_2), 3.30–3.00 (m, 4H, CH_2), 2.25–2.12 (m, 2H, CCH), 2.07–1.36 (m, 16H, CCH_2), 1.34–0.84 (m, 15H, CCH_3). ^{13}C NMR (100 MHz, MeOD): δ 174.14, 173.99, 173.08, 172.95, 171.23, 171.20, 138.83, 137.93, 130.19, 130.02, 129.76, 129.55, 128.37, 127.90, 62.85, 62.01, 60.93, 56.31, 52.89, 52.77, 51.53, 51.42, 49.64, 49.43, 49.21, 48.79, 48.57, 48.50, 48.36, 47.80, 41.90, 39.01, 38.49, 36.13, 32.36, 30.42, 29.22, 29.16, 26.51, 26.01, 25.91, 25.44, 23.98, 22.28, 22.05, 18.99, 15.69, 11.11. ESI-MS revealed that the $[M+H]^+$ (*m/z*) of compound h was 883.50, which is consistent with the theoretical molecular weight 882.51.

Samoamide A cytotoxicity test

As shown in Fig. 3, the survival rate of 4T1 cells gradually decreased with increasing of concentration of samoamide A, and when the concentration reached 50.0 μg/mL, the survival rate of 4T1 cells was only 20.79%, indicating that samoamide A had a greater effect on the survival rate of tumor cells. The result was consistent with the reported results of the natural samoamide A extracted from *Symploca* sp. (Naman et al 2017).

Effect of samoamide A on the inhibition rate of DPP4 enzyme activity

DPP4 is a key enzyme involving in allosteric-binding sites of tumor cells. The activity of tumor cells can be inhibited by inhibiting DPP4 enzyme activity. In this study, the effect of the sample on inhibiting enzyme activity was determined as the changes in the released quenched fluorescent groups when DPP4 digested the substrate.

Using sitagliptin as a control inhibitor, the effects of different concentrations of samoamide A solutions on the inhibiting DPP4 activity were investigated. The results shown in Fig. 4 suggests that the inhibition rate of DPP4 enzyme activity increased with increasing the concentration of samoamide A solution. When the concentration of samoamide A solution was 100.0 μg/mL, inhibition of

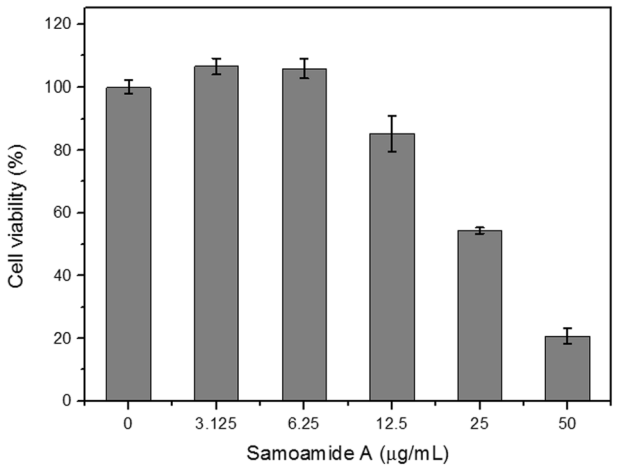

Fig. 3 Effect of different concentrations of samoamide A on cell viability. Cytotoxicity of different concentrations of samoamide A solution with 0, 3.125, 6.25, 12.5, 25, and 50 μg/mL on 4T1 cells were investigated, respectively, by CCK-8 assay in vitro

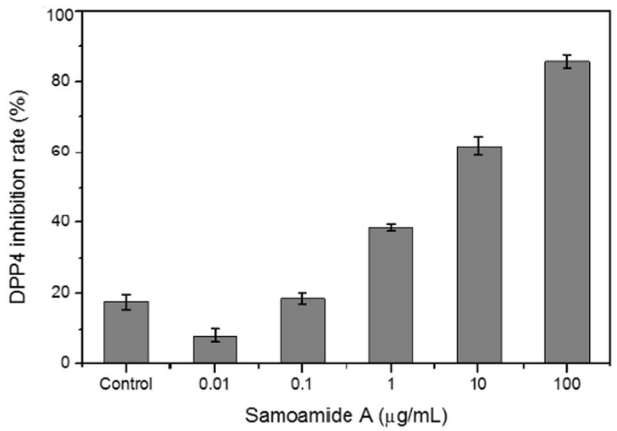

Fig. 4 Effect of different concentrations of samoamide A on enzyme inhibition rate. Using sitagliptin as a control inhibitor, the effects of samoamide A solutions at different concentrations of 0.01, 0.1, 1, 10, and 100 μg/mL on the inhibition rate of dipeptidyl peptidase-4 activity were investigated

enzyme activity reached 85.72%, which was significantly higher than that of the positive control group of sitagliptin (17.58%). This indicated that cyclic peptide samoamide A had relatively stronger inhibitory activity on DPP4 enzyme activity.

Cytotoxicity experiment of samoamide A derivatives

Based on the above results, when the concentration of samoamide A was 50 μg/mL, the solution showed strong cytotoxic effects toward tumor cells. Therefore, cytotoxicity toward 4T1 cells was investigated in samoamide A derivatives with concentrations of 50 μg/mL. The results are shown in Fig. 5.

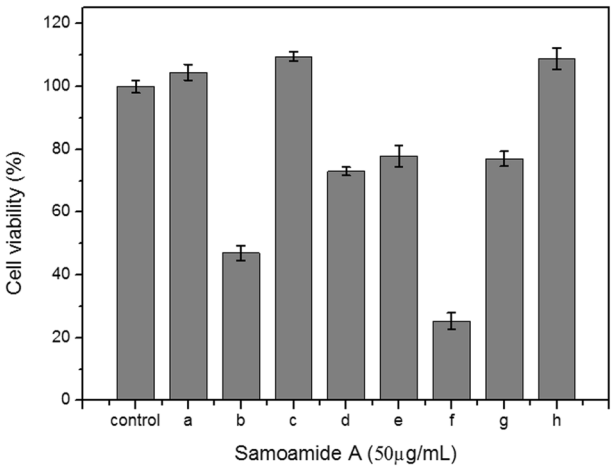

Fig. 5 Effect of 50 μg/mL samoamide A derivatives on cell viability. Cytotoxicity of samoamide A derivatives of compounds a, b, c, d, e, f, g, and h toward 4T1 cells was observed at the concentration of 50 μg/mL

Compounds a, c, and h were nontoxic to 4T1 cells; when 4T1 cells were processed with compounds d, e, and g, cell viability was >70%, which indicated that compounds d, e, and g are of low toxic in nature to 4T1 cells. The cell viability of compound b was 46.98%; the cell viability of compound f was the lowest at only 25.35%. The antitumor activities of the cyclic peptide samoamide A derivatives b and f obtained by alanine scanning were relatively closer to that (20.79%) of the procyclic peptide, in which compound f significantly inhibited the proliferation of 4T1 cells.

Effect of samoamide A derivatives on the inhibition rate of DPP4 enzyme activity

According to our results, the samoamide A at a concentration of 100 μg/mL could strongly inhibited enzyme activity. Therefore, samoamide A derivatives a, b, c, d, e, f, g, and h were performed to inhibit DPP4 enzyme activity at a concentration of 100 μg/mL, as shown in Fig. 6.

The inhibition rates of compounds a, c, and h DPP4 on enzyme activity were very low; the inhibition rates of compounds d, e, and g were all <40.0%; however, the inhibition rates of compounds b and f were higher at 81.97 and 82.44%, respectively. These values are close to the inhibition rate of 85.72% of pro-cyclic peptide, in which compound f can significantly inhibit DPP4 enzyme activity, indicating that compound f possesses strong antitumor activity.

Conclusion

Samoamide A is a new antitumor cyclic peptide extracted from *Symploca* sp., but the extraction rate is low and its

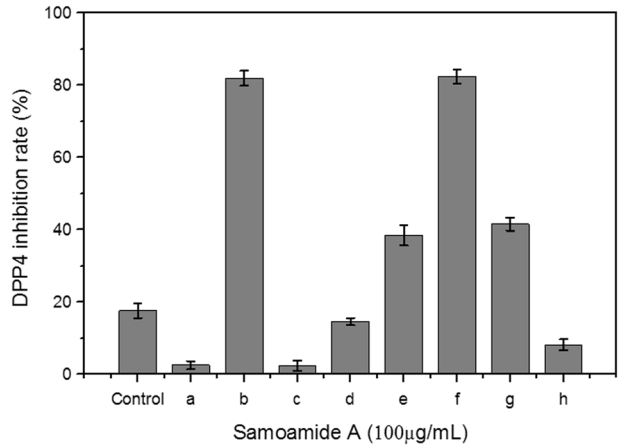

Fig. 6 Effect of 100 μg/mL samoamide A derivatives on enzyme inhibition rate. The effect of samoamide A derivatives of compound a, b, c, d, e, f, g, and h inhibiting dipeptidyl peptidase-4 enzyme activity at a concentration of 100 μg/mL was investigated

production cost is high. Samoamide A can be synthesized through cyclization of the liquid phase of the linear peptide synthesized using the Fmoc solid phase method, and the synthesis yield is 54.5%. Compared to the extraction method, the production cost is significantly reduced. Cytotoxicity and DPP4 enzyme activity inhibition experiments showed that samoamide A prepared by chemical synthesis had high antitumor activity. Based on analysis of cytotoxicity and DPP4 activity inhibition, among the eight samoamide A derivatives synthesized by the alanine scanning method, compound f showed the highest antitumor activity and its antitumor activity was closest to that of samoamide A. This indicates that proline at this site is the inactive site of samoamide A; replacement and modification of the amino acid at this site will not cause samoamide A to lose its original antitumor activity. We successfully identified the inactive site of samoamide A, which provides a theoretical basis for subsequent modification and transformation of antitumor cyclic peptide samoamide A to enhance its antitumor activity, which has high research significance and application value.

Acknowledgements This work was supported by the National Natural Science Foundation of China (NSFC) [grant number 31671797], Natural Science Foundation of Anhui University [grant number KJ2017A123, KJ2018A0117 and KZ00217058], Anhui Province Major Scientific and Technological Projects [grant number17030701014], Anhui Natural Science Foundation [grant number1808085QC85], and the Youth Talent Support Program of Anhui Polytechnic University [grant number 2016BJRRC006].

Compliance with ethical standards

Conflict of interest The authors declare that they have no conflict of interest.

Ethical approval This article does not contain any studies with human participants or animals performed by any of the authors.

Informed consent All authors listed have contributed to the conception, design, gathering, analysis or interpretation of data and have contributed to the writing and intellectual content of the article. All authors gave informed consent to the submission of this manuscript.

Publisher's note: Springer Nature remains neutral with regard to jurisdictional claims in published maps and institutional affiliations.

References

Abdalla MA (2016) Medicinal significance of naturally occurring cyclotetrapeptides. J Nat Med 70:708–720

Al-Benna S, Shai Y, Jacobsen F, Steinstraesser L (2011) Oncolytic activities of host defense peptides. Int J Mol Sci 12:8027–8051

Andrade SN, Evangelista FCG, Seckler D, Marques DR, Freitas TR, Nunes RR, Oliveira JT, RIMA Ribeiro, Santos HB, Thome RG, Taranto AG, Santos FV, GHR Viana, Freitas RP, Humberto JL, Sabino AD, Hilario FF, Varotti FP (2018) Synthesis, cytotoxic activity, and mode of action of new Santacruzamate A analogs. Med Chem Res 11-12:2397–2413

Aneiros A, Garateix A (2004) Bioactive peptides from marine sources: pharmacological properties and isolation procedures. J Chromatogr B 803:41–53

Chang Q, Li YL, Zhao X (2018) Total synthesis and cyclization strategy of samoamide A, a cytotoxic cyclic octapeptide rich in proline and phenlalanine isolated from marine cyanobacterium. J Asian Nat Prod Res https://doi.org/10.1080/10286020.2018.1450391

Dartois V, Sanchez-Quesada J, Cabezas E, Chi E, Dubbelde C, Dunn C, Granja J, Gritzen C, Weinberger D, Ghadiri MR, Parr TRJ (2005) Systemic antibacterial activity of novel synthetic cyclic peptides. Antimicrob Agents Ch49:3302–3310

Gogineni V, Hamann MT (2018) Marine natural product peptides with therapeutic potential: chemistry, biosynthesis, and pharmacology. Bba-Gen Subj 1862:81–196

Hu J, Cheng T, Zhang L, Sun B, Deng L, Xu H (2015) Anti-tumor peptide AP25 decreases cyclin D1 expression and inhibits MGC-803 proliferation via phospho-extracellular signal-regulated kinase-, Src-, c-Jun N-terminal kinase- and phosphoinositide 3-kinase-associated pathways. Mol Med Rep 12:4396–4402

Johnstone KD, Dieckelmann M, Jennings MP, Toth I, Blanchfield JT (2005) Chemo-enzymatic synthesis of a trisaccharide-linked peptide aimed at improved drug-delivery. Curr Drug Deliv 2:215–222

Khalily MP, Gerekci S, Gulec EA, Ozen C, Ozcubukcu S (2018) Structure-based design, synthesis and anticancer effect of cyclic Smac-polyarginine peptides. Amino Acids 50:1607–1616

Li CY, Gao N, Xue QQ, Ma N, Hu YQ, Zhang JF, Chen BL, Hou YC (2017) Screening and identification of a specific peptide binding to cervical cancer cells from a phage-displayed peptide library. Biotechnol Lett 39:1463–1469

Lim SS, Yoon SP, Park Y, Zhu WL, Park IS, Hahm KS, Shin SY (2006) Mechanism of antibacterial action of a synthetic peptide with an Ala-peptoid residue based on the scorpion-derived antimicrobial peptide IsCT. Biotechnol Lett 28:1431–1437

Li YZ, Zhao P, Zhan XP, Liu ZL, Mao ZM (2015) Synthesis and cytotoxic activities of novel amino acid-conjugates of pyrrole derivatives. Chin J Org Chem 35:167–174

Martin-Algarra S, Espinosa E, Rubio J, Lopez L, Juan J, Manzano JL, Carrion LA, Plazaola A, Tanovic A, Paz-Ares L (2009) Phase II

study of weekly Kahalalide F in patients with advanced malignant melanoma. Eur J Cancer Prev 45:732–735

Mccusker CF, Kocienski PJ, Boyle FT, Schatzlein AG (2002) Solid-phase synthesis of c(RGDfK) derivatives: on-resin cyclisation and lysine functionalisation. Bioorg Med Chem Lett 12:547–549

Miyake T, Loch CM, Li R (2002) Identification of a multifunctional domain in autonomously replicating sequence-binding factor 1 required for transcriptional activation, DNA replication, and gene silencing. Mol Cell Biol 22:505–516

Naman CB, Rattan R, Nikoulina SE, Lee J, Miller BW, Moss NA, Armstrong L, Boudreau PD, Debonsi HM, Valeriote FA (2017) Integrating molecular networking and biological assays to target the isolation of a cytotoxiccyclic octapeptide, samoamide A, from an American Samoan Marine Cyanobacterium. J Nat Prod 80:625–633

Oudart JB, Brassart-Pasco S, Vautrin A, Sellier C, Machado C, Dupont-Deshorgue A, Brassart B, Baud S, Dauchez M, Monboisse JC, Harakat D, Maquart FX, Ramont L (2015) Plasmin releases the anti-tumor peptide from the NC1 domain of collagen XIX. Oncotarget 6:3656–3668

Riahi N, Liberelle B, Henry O, De Crescenzo G (2017) Impact of RGD amount in dextran-based hydrogels for cell delivery. Carbohyd Polym 161:219–227

Riely GJ, Gadgeel S, Rothman I, Saidman B, Sabbath K, Feit K, Kris MG, Rizvi NA (2007) A phase 2 study of TZT-1027, administered weekly to patients with advanced non-small cell lung cancer following treatment with platinum-based chemotherapy. Lung Cancer 55:181–185

Rosca EV, Koskimaki JE, Rivera CG, Pandey NB, Tamiz AP, Popel AS (2011) Anti-angiogenic peptides for cancer therapeutics. Curr Pharm Biotechno 12:1101–1116

Schubert M, Labudde D, Oschkinat H, Schmieder P (2002) A software tool for the prediction of Xaa-Pro peptide bond conformations in proteins based on 13C chemical shift statistics. J Biomol NMR 24:149–154

Valeriote FA, Tenney K, Media J, Pietraszkiewicz H, Edelstein M, Johnson TA, Amagata T, Crews P (2012) Discovery and development of anticancer agents from marine sponges: perspectives based on a chemistry-experimental therapeutics collaborative program. J Exp Ther Oncol 10:119–134

Yi X, Yang K, Liang C, Zhong XY, Ning P, Song GS, Wang DL, Ge CC, Chen CY, Chai ZF, Liu Z (2015) Imaging-guided combined photothermal and radiotherapy to treat subcutaneous and metastatic tumors using Iodine-131-doped copper sulfide nanoparticles. Adv Funct Mater 25:4689–4699